



## Dynamical phase and quantum heat at fractional frequencies

George Thomas 

*QTF Centre of Excellence, Department of Applied Physics, Aalto University, P.O. Box 15100, FI-00076 Aalto, Finland  
and VTT Technical Research Centre of Finland Ltd, Tietotie 3, 02150 Espoo, Finland*

Jukka P. Pekola 

*QTF Centre of Excellence, Department of Applied Physics, Aalto University, P.O. Box 15100, FI-00076 Aalto, Finland*



(Received 19 July 2022; revised 28 November 2022; accepted 8 May 2023; published 22 May 2023)

We demonstrate a genuine quantum feature of heat: the power emitted by a qubit (quantum two-level system) into a reservoir under continuous driving shows peaks as a function of frequency  $f$ . These resonant features appear due to the accumulation of the dynamical phase during the driving. The position of the  $n$ th maximum is given by  $f = f_M/n$ , where  $f_M$  is the mean frequency of the qubit in the cycle, and their positions are independent of the form of the drive and the number of heat baths attached, and even the presence or absence of spectral filtering. We show that the waveform of the drive determines the intensity of the peaks, differently for odd and even resonances. This quantum heat is expected to play a crucial role in the performance of driven thermal devices such as quantum heat engines and refrigerators. We also show that, by optimizing the cycle protocol, we recover the favorable classical limit in fast driven systems without the use of counterdiabatic drive protocols, and we demonstrate an entropy preserving nonunitary process. We propose that this non-trivial quantum heat can be detected by observing the steady-state power absorbed by a resistor acting as a bolometer attached to a driven superconducting qubit.

DOI: [10.1103/PhysRevResearch.5.L022036](https://doi.org/10.1103/PhysRevResearch.5.L022036)

**Introduction.** Quantum heat transport [1–4] and quantum heat engines and refrigerators [5–8] currently attract attention because of their role in thermodynamics in the quantum domain, and their applicability in such areas as heat management in quantum circuits, qubit resetting for quantum computational tasks [9], and quantum error correction [10]. In this context, whether quantum coherence is detrimental or advantageous for the performance of the thermal machines is currently a much debated topic [8,11–21]. Moreover, the nonclassical nature of heat originates from the coherence terms of the density matrix when expressed in the eigenbasis of the Hamiltonian [22,23]. Therefore understanding the role of coherence is important: in this Letter we demonstrate the role of coherence in the emitted power by a qubit under continuous-wave high-frequency driving. In this driven open quantum system, power versus driving frequency has resonances at well-defined frequencies, due to the accumulation of the dynamical phase of the qubit [6,24–31]. In fact these peaks are general and appear irrespective of whether the qubit is coupled to the bath(s) with or without spectral filtering, and of the number of baths attached. For simplicity of obtaining transparent results, we first analyze a driven qubit coupled to a single bath, and the form of the drive is approximated by a square wave. Here we give a theoretical explanation of the

characteristics and origin of these resonances. With a single qubit, the positions of the peaks align with  $f_M/n$  dependence, where  $f_M$  is the mean frequency of the qubit in the cycle and  $n$  is an integer.

**Model.** First we consider a driven qubit coupled to a heat bath at temperature  $T$ . The Hamiltonian of the qubit is given as

$$H(t) = \frac{\hbar g \Omega(t)}{2} \sigma_z + \frac{\hbar \omega_0}{2} \sigma_x, \quad (1)$$

where  $\sigma_z$  and  $\sigma_x$  are the Pauli matrices and  $\omega_0$  is the minimum transition frequency of the qubit. Here we have the driving protocol [see Fig. 1(a)]

$$\Omega(t) = 1 + \frac{\tanh [a \cos (\omega_L t)]}{\tanh a}, \quad (2)$$

where  $\omega_L$  is the frequency,  $g$  is the amplitude of the drive and  $a$  is a real parameter. When  $a \rightarrow 0$ ,  $\Omega(t) = 1 + \cos (\omega_L t)$  and when  $a \rightarrow \infty$ ,  $\Omega(t)$  is a square wave of unit amplitude. From Eq. (1), we get the energy gap between ground and excited states of the qubit at any instant of time as

$$\Delta E(t) = \hbar \sqrt{g^2 \Omega(t)^2 + \omega_0^2}. \quad (3)$$

For  $\Omega(t) = 2$  and  $\Omega(t) = 0$ , we get maximum and minimum energy level spacings  $\Delta E_1$  and  $\Delta E_2$ , respectively. Corresponding transition frequencies are denoted as  $\omega_1 = \Delta E_1/\hbar$  and  $\omega_2 = \Delta E_2/\hbar$ . We consider a weak coupling between the system and the bath. The density matrix  $\rho$  of the system

Published by the American Physical Society under the terms of the [Creative Commons Attribution 4.0 International license](https://creativecommons.org/licenses/by/4.0/). Further distribution of this work must maintain attribution to the author(s) and the published article's title, journal citation, and DOI.

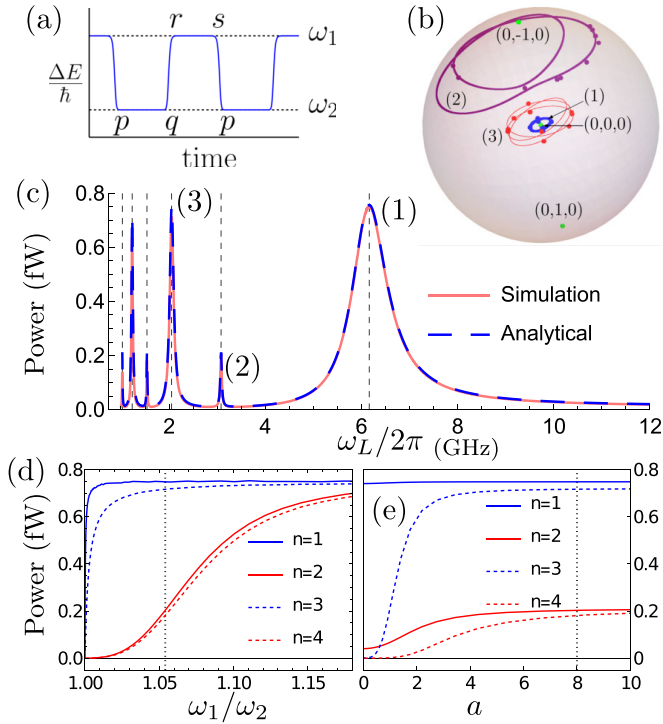


FIG. 1. (a) A pictorial representation of the driving protocol for  $a = 8$ . (b) Bloch sphere representation of the trajectories at the driving frequency  $f_{L,1}$ ,  $f_{L,2}$ , and  $f_{L,3}$ . Dots on the trajectories are obtained using Eqs. (11). (c) Power dissipated in the bath, where the red curve represents simulation using Eqs. (4), (5), and (7) and the blue dashed curve is obtained analytically from Eqs. (11) and (8). The dashed vertical lines are at  $f_{L,n}$  with  $n = 1, 2, \dots, 6$  from right to left. The peaks denoted with (1), (2), and (3) in (c) correspond to the trajectories shown in (b). Here we have ignored pure dephasing effects and taken typical parameters for a superconducting qubit:  $\omega_0/2\pi = 6$  GHz,  $g/2\pi = 1$  GHz,  $T = 70$  mK, and  $\kappa = 0.01$ . Power at the maxima of peaks of different order,  $n = 1, 2, 3, 4$ , as functions of  $\omega_1/\omega_2$  in (d) and of  $a$  in (e). The vertical dashed lines in (d) and (e) correspond to the parameter values in panel (c).

undergoes a nonunitary evolution as [32]

$$\frac{d\rho}{dt} = -\frac{i}{\hbar}[H(t), \rho] + \mathcal{L}\rho + \mathcal{L}^\phi\rho, \quad (4)$$

where the dissipator is given by

$$\begin{aligned} \mathcal{L}\rho = & \Gamma^\downarrow(\sigma^- \rho \sigma^+ - 1/2\{\sigma^- \sigma^+, \rho\}) \\ & + \Gamma^\uparrow(\sigma^+ \rho \sigma^- - 1/2\{\sigma^+ \sigma^-, \rho\}), \end{aligned} \quad (5)$$

and pure dephasing by  $\mathcal{L}^\phi\rho = \Gamma^\phi(\sigma_z \rho \sigma_z - \rho)$ . Here  $\sigma^+$  and  $\sigma^-$  are raising and lowering operators, respectively. For the case of coupling to the bath in  $\sigma_z$  direction, the transition rates are [6,8]

$$\Gamma^\downarrow = \kappa \frac{\omega_0^2}{\omega_0^2 + g^2\Omega(t)^2} \frac{\Delta E}{\hbar} [N(\Delta E) + 1]. \quad (6)$$

Here  $\kappa$  is dimensionless coupling parameter,  $N(\Delta E) = 1/[\exp(\Delta E/k_B T) - 1]$ ,  $\Gamma^\uparrow = \exp(-\Delta E/k_B T)\Gamma^\downarrow$  due to detailed balance, and from the zero frequency noise spectrum we get the pure dephasing rate as [33]  $\Gamma^\phi = \kappa[\omega_0^2/[g\Omega(t)]^2 + 1]^{-1}k_B T/\hbar$ .

*Origin of peaks in a fast driven system.* Here we analyze a case where  $\omega_0 \gg g$  in the fast driven regime  $\omega_L \gg \Gamma^\downarrow, \Gamma^\uparrow$ . We can then ignore the effects due to pure dephasing as  $g^2\Omega(t)^2 \ll \omega_0^2$ . For sufficiently large  $a$ , the drive is close to a square wave as shown in Fig. 1(a). Thus for half of the period  $\delta t = \pi/\omega_L$  the energy of the system is  $\Delta E = \Delta E_2$ , and for the other half it is  $\Delta E = \Delta E_1$  and the transitions between these legs during the drive can be approximated as sudden processes. Thus for  $a \rightarrow \infty$  baths are acting on the system only in the branches  $\Delta E = \Delta E_2$  and  $\Delta E = \Delta E_1$ , and the relaxation rates [see Eq. (6)] at these branches are denoted as  $\Gamma_2^\downarrow$  and  $\Gamma_1^\downarrow$ , respectively. Thus we can identify four steps during the drive:  $p \rightarrow q$ ,  $r \rightarrow s$  are the thermalization steps and  $q \rightarrow r$ ,  $s \rightarrow p$  represent the sudden changes as shown in Fig. 1(a). In the fast driven system, since the Hamiltonians at two different instances are not commuting  $[H(t'), H(t'')] \neq 0$ , the coherences created dissipate heat to the baths due to the work performed on the system during the driving [11]. From Eqs. (1) and (4), we get the power dissipated in the bath in a cycle as

$$P = \frac{\omega_L}{2\pi} \int_0^{2\pi/\omega_L} \text{Tr}[H(t)\mathcal{L}\rho] dt. \quad (7)$$

This expression coincides with that for the heat associated with open quantum evolution in previous literature [34–36]. For  $a \gg 1$ , we can approximate

$$P = \frac{\omega_L}{2\pi} [\Delta E_2(\mathcal{D}_q - \mathcal{D}_p) + \Delta E_1(\mathcal{D}_s - \mathcal{D}_r)], \quad (8)$$

where  $\mathcal{D}_i = 1/2 - \rho_{ee,i}$ , with  $\rho_{ee,i}$  the occupational probability of the excited state at the  $i$ th position of the cycle. Interestingly, the power versus driving frequency shows maxima, as depicted in Fig. 1(c). To explain this, we consider the dynamical phase  $\varphi$  accumulated in the off-diagonal (coherence) terms of the density matrix, which is in the form  $\exp(-i\varphi)$ , where

$$\varphi = \frac{1}{\hbar} \int_0^{2\pi/\omega_L} \Delta E(t) dt = (\Delta E_1 + \Delta E_2) \frac{\pi}{\omega_L}, \quad (9)$$

valid for any value of  $a$ . When the accumulated phase  $\varphi = 2n\pi$ , where  $n$  is an integer, the system makes  $n$  complete rotations in a Bloch sphere. Equating  $(\Delta E_1 + \Delta E_2)\pi/\hbar\omega_L = 2n\pi$ , we get the condition of these frequencies,

$$f_{L,n} = \frac{f_M}{n}, \quad (10)$$

where  $f_M = (\Delta E_1 + \Delta E_2)/2h$ . For each  $n$ , the system undergoes a trajectory with  $n$  closed loops [see Fig. 1(b)]. An immediate consequence of Eq. (9) is that the positions of the peaks are robust irrespective of the waveform of the drive.

Equation (10) can also be achieved by considering the time evolution of the density matrix in a fast driven system, as we will now demonstrate. We find an analytical expression for the density matrix and the dissipated power in the limit  $a \rightarrow \infty$ , i.e., for the abrupt changes of the energy of the qubit. We define  $\mathcal{R}_i$  and  $\mathcal{I}_i$  as the real and imaginary parts of the off-diagonal terms of the density matrix of the system, respectively. These are defined in the instantaneous eigenstates of the Hamiltonian. Their evolution can be obtained by applying the sudden approximation of quantum mechanics in legs  $q \rightarrow r$

and  $s \rightarrow p$  and relaxation in legs  $p \rightarrow q$  and  $r \rightarrow s$ . In steady state they evolve as

$$\begin{aligned}
 \mathcal{D}_q &= \mathcal{D}_p + [\Gamma_2^\downarrow - \Gamma_2^\Sigma (\mathcal{D}_p + 1/2)] \delta t_2, \\
 \mathcal{R}_q &= [\mathcal{R}_p \cos(\omega_2 \delta t_2) - \mathcal{I}_p \sin(\omega_2 \delta t_2)] (1 - \frac{1}{2} \Gamma_2^\Sigma \delta t_2), \\
 \mathcal{I}_q &= [\mathcal{I}_p \cos(\omega_2 \delta t_2) + \mathcal{R}_p \sin(\omega_2 \delta t_2)] (1 - \frac{1}{2} \Gamma_2^\Sigma \delta t_2) = \mathcal{I}_r, \\
 \mathcal{D}_r &= \sqrt{1 - \eta^2} \mathcal{D}_q - \eta \mathcal{R}_q, \quad \mathcal{R}_r = \sqrt{1 - \eta^2} \mathcal{R}_q + \eta \mathcal{D}_q, \\
 \mathcal{D}_s &= \mathcal{D}_r + [\Gamma_1^\downarrow - \Gamma_1^\Sigma (\mathcal{D}_r + 1/2)] \delta t_1, \\
 \mathcal{R}_s &= [\cos(\omega_1 \delta t_1) \mathcal{R}_r - \mathcal{I}_q \sin(\omega_1 \delta t_1)] (1 - \frac{1}{2} \Gamma_1^\Sigma \delta t_1), \\
 \mathcal{I}_s &= [\cos(\omega_1 \delta t_1) \mathcal{I}_q + \mathcal{R}_r \sin(\omega_1 \delta t_1)] (1 - \frac{1}{2} \Gamma_1^\Sigma \delta t_1) = \mathcal{I}_p, \\
 \mathcal{D}_p &= \sqrt{1 - \eta^2} \mathcal{D}_s + \eta \mathcal{R}_s, \quad \mathcal{R}_p = \sqrt{1 - \eta^2} \mathcal{R}_s - \eta \mathcal{D}_s. \quad (11)
 \end{aligned}$$

Here we consider  $\Gamma_1^\Sigma \delta t_1 \ll 1$  and  $\Gamma_2^\Sigma \delta t_2 \ll 1$ , where  $\Gamma_{1(2)}^\Sigma = \Gamma_{1(2)}^\uparrow + \Gamma_{1(2)}^\downarrow$  and  $\delta t_1$  and  $\delta t_2$  are the durations of the legs  $p \rightarrow q$  and  $r \rightarrow s$ , respectively, such that  $\omega_L = 2\pi/(\delta t_1 + \delta t_2)$ , and  $\eta = \sqrt{1 - \omega_2^2/\omega_1^2}$ . For the symmetric case  $\delta t_1 = \delta t_2$ , Eqs. (11) represent the evolution of the system corresponding to the driving protocol in Eqs. (1) and (2) with  $a \rightarrow \infty$ , and below we show that it yields identical results with the full numerical solution of the master equation [Eq. (4)]. Naturally the maximum occupation probability of the excited state at the point  $p$  versus driving frequency appears at the same position as that of power maxima shown in Fig. 1(c). From Eqs. (11), and considering  $\Gamma_1^\downarrow = \Gamma_1^\Sigma = 0$ ,  $\delta t_2 = \delta t_1 = \delta t$  and  $\Gamma_2^\downarrow \delta t \ll 1$ , we get

$$P = \frac{\Delta E_2 (2\Gamma_2^\downarrow - \Gamma_2^\Sigma) [1 - \cos(\omega_1 \delta t)] (\omega_1^2 - \omega_2^2)}{2(4\omega_1^2 - (\omega_1 + \omega_2)^2 \cos[(\omega_2 + \omega_1) \delta t] - \mathcal{K})} \quad (12)$$

and

$$\begin{aligned}
 \rho_{ee,p} &= \frac{1}{2} - \frac{(2\Gamma_2^\downarrow - \Gamma_2^\Sigma)}{\Gamma_2^\Sigma} \\
 &\times \frac{4[\omega_1 \cos \frac{\omega_1 \delta t}{2} \sin \frac{\omega_2 \delta t}{2} + \omega_2 \cos \frac{\omega_2 \delta t}{2} \sin \frac{\omega_1 \delta t}{2}]^2}{(4\omega_1^2 - (\omega_1 + \omega_2)^2 \cos[(\omega_2 + \omega_1) \delta t] - \mathcal{K})}, \quad (13)
 \end{aligned}$$

with  $\mathcal{K} = 2(\omega_1^2 - \omega_2^2) \cos[\omega_2 \delta t] + (\omega_1 - \omega_2)^2 \cos[(\omega_1 - \omega_2) \delta t]$ . The analytical results above are valid for small amplitude ( $\omega_1 \approx \omega_2$ ), square-wave driving ( $a \rightarrow \infty$ ) of the qubit. It is, however, illustrative to look at different driving protocols to understand the various peaks and their origin. In Fig. 1(d), the amplitudes of the various peaks are presented against  $\omega_1/\omega_2$ . We see that the odd  $n$  peaks assume their asymptotic value already with weak driving, whereas the even  $n$  peaks grow more gradually. This is in line with the results in panels (b) and (c), where the even peaks behave very differently (on the Bloch sphere, and in terms of the height and width of the peaks) with respect to odd  $n$  peaks. In Fig. 1(e) the same quantities are plotted now as functions of  $a$ . Only the  $n = 1$  peak survives all the way to  $a \rightarrow 0$ , i.e., for a sinusoidal drive, whereas the rest of the peaks arise only for non-vanishing  $a$ . This observation suggests that the magnitude of the  $n$ th peak is determined by the corresponding Fourier component of the drive.

When  $\omega_1 \rightarrow \omega_2$ , we get from Eqs. (12) and (13) maximum values for  $P$  and  $\rho_{ee,p}$  for  $\delta t = 2n\pi/(\omega_2 + \omega_1)$ , which corresponds to Eq. (10) and to the peaks obtained in the power. The condition used in Eqs. (12) and (13),  $\Gamma_1^\downarrow = \Gamma_1^\Sigma = 0$ , can be easily achieved by using spectral filter with sufficiently high quality factor [3]. Interestingly, when  $\delta t = 2n\pi/\omega_1$ ,  $P = 0$ , and  $\rho_{ee,p} = \Gamma_2^\uparrow/\Gamma_2^\Sigma$ , which is the classical limit [6]. In this case,  $\mathcal{R}_r = \mathcal{R}_s$ ,  $\mathcal{I}_r = \mathcal{I}_s$ , and  $\mathcal{D}_r = \mathcal{D}_s$  due to which the coherence created during the ramp  $q \rightarrow r$  is annihilated in the ramp  $s \rightarrow p$ . Generally, transitionless quantum driving is achieved by counterdiabatic driving [37,38]. Here, we achieve the classical limit with minimal power without such counterdiabatic driving but with suitable choice of the driving protocol.

Another implication of  $\Gamma_1^\downarrow = \Gamma_1^\Sigma = 0$  is that the nonunitary step where the system is in contact with the heat bath should preserve the purity of the qubit. Consider  $U_{ij}$  as the unitary process representing the ramp  $i \rightarrow j$  where  $i, j = \{p, q, r, s\}$ . From the cyclic process described in Fig. 1(a), we have

$$\mathcal{V}_{pq}\{U_{sp}U_{rs}U_{qr}\rho_q U_{qr}^\dagger U_{rs}^\dagger U_{sp}^\dagger\} = \rho_q, \quad (14)$$

where  $\rho_q$  is the density matrix at the beginning of the ramp  $q \rightarrow r$  and  $\mathcal{V}_{pq}$  represents the map corresponding to nonunitary process in the branch  $p \rightarrow q$ . Unitary processes preserve the von Neumann entropy (purity) of the system. To achieve cyclicity as shown in Eq. (14), purity of the system in nonunitary branch  $p \rightarrow q$  should also be preserved. This implies

$$\mathcal{D}_i^2 + \mathcal{R}_i^2 + \mathcal{I}_i^2 = \mathcal{D}_j^2 + \mathcal{R}_j^2 + \mathcal{I}_j^2. \quad (15)$$

Under Lindblad evolution, due to decoherence, we have  $\sqrt{\mathcal{R}_q^2 + \mathcal{I}_q^2} < \sqrt{\mathcal{R}_p^2 + \mathcal{I}_p^2}$ , which implies  $\mathcal{D}_q > \mathcal{D}_p$  and thereby  $P > 0$  as expected. A possible application of this effect can be mitigation of the loss of quantum information in an open system with drive.

*Bloch sphere dynamics.* The driven system shows interesting trajectories in the Bloch sphere representation. The coordinates of the Bloch vector at a given instant of time are  $(\langle \sigma_x \rangle_t, \langle \sigma_y \rangle_t, \langle \sigma_z \rangle_t)$  where  $\langle \sigma_i \rangle_t = \text{Tr}[\sigma_i \rho(t)]$  and  $\rho(t)$  is obtained from Eq. (4) for  $t \rightarrow \infty$ . Since we are depicting steady state cyclic processes, all the trajectories in the Bloch sphere for a complete cycle should be closed. Depending on the driving frequency or in other words, the position of the peak, the number of turns in the Bloch sphere trajectory equals  $n$  [see Fig. 1(b)]. For driving frequencies away from  $f_M/n$ , the trajectories are close to the surface [not shown in Fig. 1(b)]. They move towards the center of the Bloch sphere when the driving frequencies are close to  $f_M/n$  (peaks). This is due to the fact that at driving frequencies near  $f_{L,n}$  the off diagonal coherence terms are created which then dissipate to the bath. Or in other words, the driving increases the entropy which in turn increases the mixedness of the system. Thus trajectories reflect the amount of dissipation. The trajectory on the Bloch sphere can also be constructed from Eqs. (11). At a given instant, the coordinates are  $2(\mathcal{R}, \mathcal{I}, \mathcal{D})$ . As an example, we represent the state of the system obtained from Eqs. (11) at a few instances as dots in Fig. 1(b). This shows an excellent agreement between analytical solution from Eqs. (11) and numerical simulations.

*Experimental setup.* The predicted quantum heat might be observable in a basic qubit based setup. For a transmon qubit

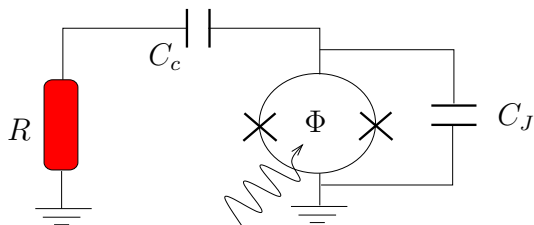


FIG. 2. A possible experimental setup consists of a superconducting qubit capacitively coupled to a normal metal resistor with resistance  $R$ .

[39] with  $\Delta E = \hbar\omega$ , coupled to a resistor as bath [40] through a capacitor with capacitance  $C_c$  (see Fig. 2), the transition rate is given as

$$\Gamma^\downarrow = \frac{\omega_0^2}{\omega_0^2 + g^2\Omega(t)^2} \frac{C_c^2}{C_\Sigma^2} \frac{\omega}{Q} [N(\Delta E) + 1], \quad (16)$$

where  $C_J$  is the capacitance of each junction,  $C_\Sigma = C_c + 2C_J$ , the quality factor of the junction  $Q = \sqrt{L_J/C_J}/R = 1/\omega C_J R$ , and  $L_J$  is the Josephson inductance which can be modulated with flux  $\Phi$ . For  $g\Omega(t)/\omega_0 \ll 1$  and for low temperature  $\hbar\omega > k_B T$ , we get

$$\Gamma^\downarrow \approx C_c^2 C_J (C_J + C_c)^{-2} \omega^2 R C_J. \quad (17)$$

For typical values of a transmon,  $C_J = 30$  fF,  $C_c = 8$  fF,  $\omega/2\pi = 6$  GHz, and  $R = 200$   $\Omega$ , we have  $\Gamma^\downarrow/\omega \approx 0.01$ , which represents weak coupling and the proposed model is applicable.

**Cooling regime** We have seen that the classical limit or in other words suppression of the coherence induced dissipation, can be achieved by considering  $\Gamma_1^\downarrow = \Gamma_1^\uparrow = 0$  and  $\delta t = 2n\pi/\omega_1$ . We can extend this approach for two baths coupled to the qubit via resonators to approach this limit. Such a setup will be useful in constructing quantum heat engines and refrigerators [31]. The resonators (spectral filters) will help to couple the qubit to the bath 1 with temperature  $T_1$  when  $\Delta E = \Delta E_1$  and to the bath 2 at temperature  $T_2$  when  $\Delta E = \Delta E_2$ , and allow almost unitary evolution in between as discussed in Refs. [3,8]. Now we find the power dissipated to baths 1 and 2 as  $P_1 = [\Delta E_1(\mathcal{D}_s - \mathcal{D}_r)]\omega_L/2\pi$  and  $P_2 = [\Delta E_2(\mathcal{D}_q - \mathcal{D}_p)]\omega_L/2\pi$ , respectively. The cooling regime is defined as  $P_2 < 0$  and  $P_1 > 0$  and can be achieved at high frequency by suitably choosing  $\delta t_2$  and  $\delta t_1$ . If we consider the case  $\delta t_2 = \pi/\omega_2$ , we get cooling for  $\delta t_1 = 2n\pi/\omega_1$  as shown in Fig. 3. The transition rate due to the bath in the presence of resonators is given as [6]

$$\Gamma_r^\downarrow = \kappa \frac{\omega_0^2}{\omega_0^2 + g^2\tilde{\Omega}(t)^2} \frac{[N(\Delta E) + 1]\Delta E/\hbar}{1 + Q_r^2\left(\frac{\omega_r}{\omega} - \frac{\omega}{\omega_r}\right)^2}, \quad (18)$$

where  $r = 1, 2$ ,  $Q_r$  is the quality factor of the  $r$ th resonator,  $\omega = \Delta E/\hbar$ , and  $\tilde{\Omega}(t)$  corresponds to the drive shown in the inset of Fig. 3(a). Moreover, the dynamical phase is  $\varphi = \frac{1}{\hbar} \int_0^{2\pi/\omega_L} \Delta E(t) dt = \pi + \omega_1(2\pi/\omega_L - \pi/\omega_2)$ . Invoking the condition  $\varphi = 2n\pi$  as in Eq. (10), we get the power maxima (see Fig. 3) at frequencies

$$f_{L,n}^{\text{asy}} = \frac{1}{2\pi} \frac{2\omega_2\omega_1}{(2n-1)\omega_2 + \omega_1}. \quad (19)$$

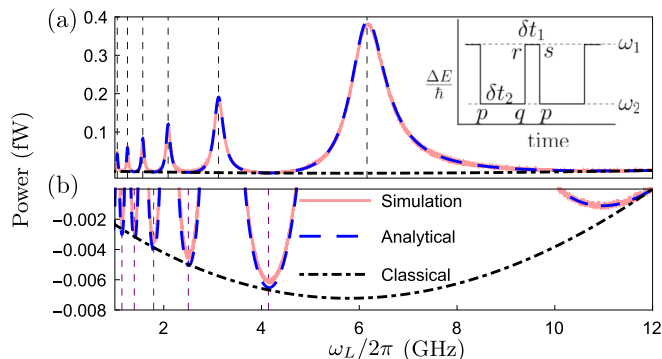


FIG. 3. (a) Power  $P_2$  versus frequency. Panel (b) shows the enlarged cooling regime. The inset shows the asymmetric square-wave driving protocol ( $\delta t_2 \neq \delta t_1$ ) used in (a) and (b). The dashed blue and continuous red curves correspond to theoretical model from Eqs. (11) and simulation, respectively. The dot-dashed black curves indicate the classical limit with same energy level spacings and transition rates as in the quantum system. Vertical dashed lines in (a) are obtained from Eq. (19). Here  $\omega_L$  is varied by changing  $\delta t_1$ . The vertical dashed lines in (b) correspond to  $\delta t_1 = 2n\pi/\omega_1$ , where cooling is achieved. We take  $\delta t_2 = \pi/\omega_2$ ,  $T_1 = T_2 = 210$  mK,  $\omega_0/2\pi = 6$  GHz,  $g/2\pi = 1$  GHz, and  $\kappa = 0.01$ .

The validity of Eqs. (11) is in the regime  $\Gamma_1^\downarrow \delta t_1 \ll 1$  and  $\Gamma_2^\downarrow \delta t_2 \ll 1$ , because we consider only the linear terms in  $\delta t_1$  and  $\delta t_2$  in the dissipators [see Eqs. (5) and (11)] in branches  $p \rightarrow q$  and  $r \rightarrow s$ . Therefore we can see a slight mismatch between simulation and analytical solution in Fig. 3.

Irrespective of the initial state of the system, after sufficiently many periods of drive, the system reaches a *steady state cycle* with the same trajectory in the Bloch sphere for all the subsequent cycles. At this point, interesting questions in the periodically driven open quantum system are, what would be the minimum relaxation rate required to make the evolution of the system cyclic [41] and what would be the corresponding trajectory since for fully unitary (closed system) such steady state is not reached? This can be understood from Eqs. (11) and (13). For  $\Gamma_1^\downarrow = 0$ , the cyclic condition is satisfied for any  $\Gamma_2^\downarrow$  except for  $\Gamma_2^\downarrow = 0$ . As  $\Gamma_2^\downarrow \rightarrow 0$ , the cyclic trajectory of the system approaches the center of the Bloch sphere. So in Eq. (13) we get  $\rho_{ee,p} \rightarrow 1/2$  and thereby  $\mathcal{D}_p \rightarrow 0$ . Similar analysis can be done for  $\mathcal{R}$  and  $\mathcal{I}$ . As  $\Gamma_2^\downarrow \rightarrow 0$ , the Bloch vector  $2(\mathcal{R}, \mathcal{I}, \mathcal{D}) \rightarrow (0, 0, 0)$ . Thus, for an arbitrary initial state away from the steady state trajectory, the system takes infinitely many cycles for  $\Gamma_2^\downarrow \rightarrow 0$  to reach the steady state cycle. But for any non-vanishing  $\Gamma_2^\downarrow$ , a steady state cycle is eventually reached.

To conclude, we have established the relation between the quantum heat in driven systems and the dynamical phase acquired during the drive. We show that odd and even peaks of quantum heat have different origins and their intensity depends on the waveform of the drive. By manipulating the cycle protocol, one can approach the favorable classical limit without counterdiabatic drive and it is possible to preserve purity even in the presence of a heat bath. We discussed the trajectories traversed by the qubit on the Bloch sphere and the impact of dissipation on cyclicity. Our work

can be extended to many interesting directions such as experimental verification of the proposed model, analysis of whether the system can outperform the classical limit, and heat transport at other fractional frequencies in multilevel systems.

*Acknowledgments.* We thank Bayan Karimi and Dmitry S. Golubev for useful discussions. We acknowledge Academy

of Finland Grant No. 312057, the European Union's Horizon 2020 research and innovation program under the European Research Council (ERC) program (Grant No. 742559), and the Foundational Questions Institute Fund (FQXi) via Grant No. FQXi-IAF19-06. G.T. also acknowledge the support by the Academy of Finland Flagship Programme, Photonics Research and Innovation (PREIN), Decision No. 320168.

- 
- [1] N. Li, J. Ren, L. Wang, G. Zhang, P. Hänggi, and B. Li, Colloquium: Phononics: Manipulating heat flow with electronic analogs and beyond, *Rev. Mod. Phys.* **84**, 1045 (2012).
- [2] Y. Dubi and M. Di Ventra, Colloquium: Heat flow and thermoelectricity in atomic and molecular junctions, *Rev. Mod. Phys.* **83**, 131 (2011).
- [3] A. Ronzani, B. Karimi, J. Senior, Y.-C. Chang, J. T. Peltonen, C. Chen, and J. P. Pekola, Tunable photonic heat transport in a quantum heat valve, *Nat. Phys.* **14**, 991 (2018).
- [4] J. P. Pekola and B. Karimi, Colloquium: Quantum heat transport in condensed matter systems, *Rev. Mod. Phys.* **93**, 041001 (2021).
- [5] S. Vinjanampathy and J. Anders, Quantum thermodynamics, *Contemp. Phys.* **57**, 545 (2016).
- [6] B. Karimi and J. P. Pekola, Otto refrigerator based on a superconducting qubit: Classical and quantum performance, *Phys. Rev. B* **94**, 184503 (2016).
- [7] S. Deffner and S. Campbell, *Quantum Thermodynamics*, (Morgan and Claypool, San Rafael, CA, 2019).
- [8] J. P. Pekola, B. Karimi, G. Thomas, and D. V. Averin, Supremacy of incoherent sudden cycles, *Phys. Rev. B* **100**, 085405 (2019).
- [9] K. Y. Tan, M. Partanen, R. E. Lake, J. Govenius, S. Masuda, and M. Möttönen, Quantum-circuit refrigerator, *Nat. Commun.* **8**, 15189 (2017).
- [10] A. Danageozian, M. M. Wilde, and F. Buscemi, Thermodynamic constraints on quantum information gain and error correction: A triple trade-off, *PRX Quantum* **3**, 020318 (2022).
- [11] R. Kosloff and T. Feldmann, Discrete four-stroke quantum heat engine exploring the origin of friction, *Phys. Rev. E* **65**, 055102(R) (2002).
- [12] M. O. Scully, M. S. Zubairy, G. S. Agarwal, and H. Walther, Extracting Work from a single heat bath via vanishing quantum coherence, *Science* **299**, 862 (2003).
- [13] M. O. Scully, K. R. Chapin, K. E. Dorfman, M. B. Kim, and A. Svidzinsky, Quantum heat engine power can be increased by noise-induced coherence, *Proc. Natl. Acad. Sci. USA* **108**, 15097 (2011).
- [14] K. Brandner and U. Seifert, Periodic thermodynamics of open quantum systems, *Phys. Rev. E* **93**, 062134 (2016).
- [15] A. Streltsov, G. Adesso, and M. B. Plenio, Colloquium: Quantum coherence as a resource, *Rev. Mod. Phys.* **89**, 041003 (2017).
- [16] J.-Y. Du and F.-L. Zhang, Nonequilibrium quantum absorption refrigerator, *New J. Phys.* **20**, 063005 (2018).
- [17] M. Kilgour and D. Segal, Coherence and decoherence in quantum absorption refrigerators, *Phys. Rev. E* **98**, 012117 (2018).
- [18] V. Holubec and T. Novotný, Effects of noise-induced coherence on the performance of quantum absorption refrigerators, *J. Low Temp. Phys.* **192**, 147 (2018).
- [19] P. A. Camati, J. F. G. Santos, and R. M. Serra, Coherence effects in the performance of the quantum Otto heat engine, *Phys. Rev. A* **99**, 062103 (2019).
- [20] K. Hammam, Y. Hassouni, R. Fazio, and G. Manzano, Optimizing autonomous thermal machines powered by energetic coherence, *New J. Phys.* **23**, 043024 (2021).
- [21] R. Dann and R. Kosloff, Quantum signatures in the quantum Carnot cycle, *New J. Phys.* **22**, 013055 (2020).
- [22] C. Elouard, D. A. Herrera-Martí, M. Clusel, and A. Auffèves, The role of quantum measurement in stochastic thermodynamics, *npj Quantum Inf.* **3**, 9 (2017).
- [23] C. Elouard, G. Thomas, O. Maillet, J. P. Pekola, and A. N. Jordan, Quantifying the quantum heat contribution from a driven superconducting circuit, *Phys. Rev. E* **102**, 030102(R) (2020).
- [24] M. Grifoni and P. Hänggi, Driven quantum tunneling, *Phys. Rep.* **304**, 229 (1998).
- [25] M. Carrega, P. Solinas, M. Sassetti, and U. Weiss, Energy Exchange in Driven Open Quantum Systems at Strong Coupling, *Phys. Rev. Lett.* **116**, 240403 (2016).
- [26] A. Russomanno, A. Silva, and G. E. Santoro, Periodic Steady Regime and Interference in a Periodically Driven Quantum System, *Phys. Rev. Lett.* **109**, 257201 (2012).
- [27] A. Russomanno and G. E. Santoro, Floquet resonances close to the adiabatic limit and the effect of dissipation, *J. Stat. Mech.* (2017) 103104.
- [28] M. P. Silveri, K. S. Kumar, J. Tuorila, J. Li, A. Vepsäläinen, E. V. Thuneberg and G. S. Paroanu, Stückelberg interference in a superconducting qubit under periodic latching modulation, *New J. Phys.* **17**, 043058 (2015).
- [29] S. N. Shevchenko and A. N. Omelyanchouk, Multiphoton transitions in Josephson-junction qubits (Review Article), *Low Temp. Phys.* **38**, 283 (2012).
- [30] U. Mishra and A. Bayat, Driving Enhanced Quantum Sensing in Partially Accessible Many-Body Systems, *Phys. Rev. Lett.* **127**, 080504 (2021).
- [31] A. Guthrie, C. Dimas Satrya, Yu.-C. Chang, P. Menczel, F. Nori, and J. P. Pekola, Cooper-Pair Box Coupled to Two Resonators: An Architecture for a Quantum Refrigerator, *Phys. Rev. Appl.* **17**, 064022 (2022).
- [32] H. P. Breuer and F. Petruccione, *The Theory of Open Quantum Systems* (Oxford University Press, Oxford, 2002).
- [33] C. Xu, A. Poudel, and M. G. Vavilov, Nonadiabatic dynamics of a slowly driven dissipative two-level system, *Phys. Rev. A* **89**, 052102 (2014).

- [34] R. Alicki, The quantum open system as a model of the heat engine, *J. Phys. A: Math. Gen.* **12**, L103 (1979).
- [35] P. Solinas, D. V. Averin, and J. P. Pekola, Work and its fluctuations in a driven quantum system, *Phys. Rev. B* **87**, 060508(R) (2013).
- [36] M. Esposito, U. Harbola, and S. Mukamel, Nonequilibrium fluctuations, fluctuation theorems, and counting statistics in quantum systems, *Rev. Mod. Phys.* **81**, 1665 (2009).
- [37] M. Demirplak and S. A. Rice, Adiabatic population transfer with control fields, *J. Phys. Chem. A* **107**, 9937 (2003).
- [38] M. V. Berry, Transitionless quantum driving, *J. Phys. A: Math. Theor.* **42**, 365303 (2009).
- [39] J. Koch, T. M. Yu, J. Gambetta, A. A. Houck, D. I. Schuster, J. Majer, A. Blais, M. H. Devoret, S. M. Girvin, and R. J. Schoelkopf, Charge-insensitive qubit design derived from the Cooper pair box, *Phys. Rev. A* **76**, 042319 (2007).
- [40] H. Nyquist, Thermal agitation of electric charge in conductors, *Phys. Rev.* **32**, 110 (1928).
- [41] P. Menczel and K. Brandner, Limit cycles in periodically driven open quantum systems, *J. Phys. A: Math. Theor.* **52**, 43LT01 (2019).